Two-dimensional ion trap lattice on a microchip for quantum simulation

R. C. Sterling,[1] H. Rattanasonti,[2] S. Weidt,[1] K. Lake,[1] P. Srinivasan,[2] S. C. Webster,[1] M. Kraft,[2] and W. K. Hensinger[1]

[1]*Department of Physics and Astronomy, University of Sussex, Brighton, BN1 9QH, UK*
[2]*School of Electronics and Computer Science, University of Southampton, Highfield, Southampton, UK, SO17 1BJ*

Using a controllable quantum system it is possible to simulate other highly complex quantum systems efficiently overcoming an in-principle limitation of classical computing. Trapped ions constitute such a highly controllable quantum system. So far, no dedicated architectures for the simulation of two-dimensional spin lattices using trapped ions in radio-frequency ion traps have been produced, limiting the possibility of carrying out such quantum simulations on a large scale. We report the operation of a two-dimensional ion trap lattice integrated in a microchip capable of implementing quantum simulations of two-dimensional spin lattices. Our device provides a scalable microfabricated architecture for trapping such ion lattices with coupling strengths between neighbouring ions sufficient to provide a powerful platform for the implementation of quantum simulations. In order to realize this device we developed a specialist fabrication process that allows for the application of very large voltages. We fabricated a chip containing an array of microtraps forming a closely spaced ion lattice. We demonstrate reliable trapping of a lattice of ytterbium ions, measure long ion lifetimes and show the lattice is suitable for performing quantum simulations. We are also able to deterministically introduce defects into the lattice adding further classes of quantum simulations that can be performed. Additionally, we demonstrate rudimentary shuttling of single ions between neighbouring lattice sites. The successful operation of this device provides a powerful tool to obtain a new understanding of many quantum systems in nature. Another step-changing application of this device consists of the generation of two-dimensional cluster states for measurement-based quantum computing.

An analog quantum simulator is a device in which the Hamiltonian of a complicated many-body system can be realized and its properties measured. Such a device would enable investigation of quantum phenomena currently beyond that of classical computation or direct measurement [1]. The applications for a quantum simulator are numerous and far reaching, including, among others, the simulation of quantum magnetism, high-temperature superconductivity, fractional quantum Hall effect and synthetic gauge fields [2–5]. Quantum simulations may revolutionize our understanding of many-body systems.

Proof of principle analog quantum simulators have already been demonstrated using ultra-cold quantum gases [6], photons [7], trapped ions [8] and NMR [9]. Of the various systems trapped ions are one of the most promising due to the demonstration of unparalleled quantum control and isolation from the environment [10].

While some seminal small scale quantum simulations have been performed within radio-frequency (rf) ion traps [11–17], they suffer limitations when trying to scale to a larger number of particles. The harmonic potential along the weak axis can result in varying ion-ion separations and coupling rates. Furthermore, ions at the rf nil naturally form a 1-dimensional string making the simulation of arbitrary lattice geometries experimentally demanding [18]. A 2D Ising-type interaction has been observed with Penning traps [19], but the rotating crystal makes individual ion addressing and readout experimentally challenging, and the lattice geometry is limited to the naturally forming Wigner crystal.

A different approach constitutes the proposal to use a two-dimensional lattice of rf ion traps [20–22]. Each lattice site contains a single ion which interacts with neighboring ions via the Coulomb force. To date, experimental progress towards such a lattice has been limited to trapping dust particles and ion clouds above PCB boards [23] or wire meshes [24]. Here, we report on the microfabrication of a lattice of ion traps on a microchip and demonstrate trapping of a lattice of single Yb^+ ions, the deterministic generation of lattice defects and rudimentary ion shuttling between lattice sites. Additionally to being suitable for quantum simulation this microchip offers a suitable architecture for 2D cluster state generation [25] and a possible avenue for the development of quantum information processing [20]. As our device is an ion trap chip [26] it is scalable to much larger ion lattices.

The layered structure of a commercial silicon-on-insulator (SOI) wafer was used to fabricate a 2.5D ion trap, with recessed ground electrodes within a 2D electrode geometry, shown in Fig. 1A and B, in a fabrication process similar to that used by Britton *et al.* [27]. The microchip consists of 29 traps arranged in a triangular lattice, with each ion having up to six nearest neighbors with an ion-ion separation of 270.5

μm. The ion-electrode separation is 156 μm. Due to the recessed ground electrodes the ion height from the top of the trap surface is 116 μm, as seen in Fig. 1C.

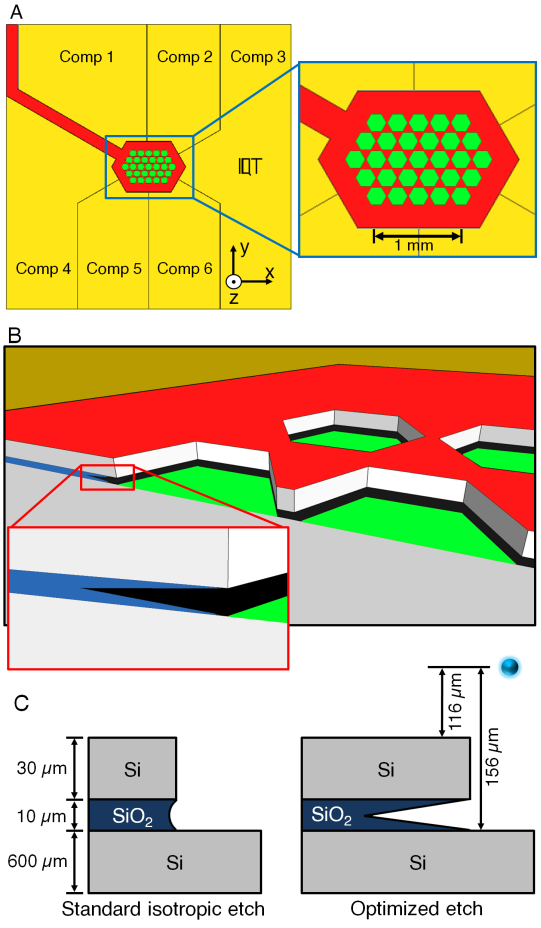

Figure 1: (**A**) The electrode design for the microchip. The rf electrode is shown in red, compensation electrodes are shown in gold and the ground electrode is shown in green. (**B**) Cross-section drawing of the trap geometry, showing the SOI layered geometry. The close-up inset shows the deep V undercut achievable with our fabrication process. (**C**) Two schematics of the etch profile, a typical isotropic etch is shown on the left, showing a slight undercut into the buried oxide. The right picture shows the profile of our optimized etch. The preferential etch rate along the bond face results in a deep V-shaped undercut. The ion height relative to the trap electrodes is also shown.

In operating a microfabricated ion trap, restrictions on the rf voltage that can be applied limit trap depth and require small ion-electrode distances. Low flashover voltages have been a problem in previously reported microfabricated ion traps [26, 28], limiting obtainable ion life times and secular frequencies. To ensure efficient operation of our lattice ion trap we have designed a fabrication process to allow for high voltages, greatly reducing constraints on the trap design. Firstly, a thick oxide layer was chosen, this increases the path length between the electrodes and the handle layer as well as reducing capacitance between the rf electrode and ground. This aids the application of high rf voltages via a high Q helical coil resonator. The SOI structure was fabricated by wafer bonding two wafers with 5 μm thick oxide surfaces to form a 10 μm thick buried oxide layer. Such a bonded substrate allows the deep undercut seen in our microchip. This occurs as there is an increased etch rate on this interface resulting in an anisotropic etch laterally under the electrodes. Using a buffered HF etch, lasting approximately $130 - 140$ minutes, the oxide layer was removed to expose the handle layer and producing the V-shaped undercut. The lateral undercut measured in our fabrication is approximately 60 μm, as seen in Fig. 2B. This V-shaped etch profile substantially increases the path length between the electrodes and ground resulting in extremely high breakdown voltages as it increases the effective distance for surface flashover from 10 μm to up to 120 μm. Electrical flashover measurements were performed on SOI test samples to determine the voltage that can be applied (see Sterling *et al.* [29] for a technical description of how the flashover measurements are carried out). The flashover voltages were measured to be $V_{dc} = 1298(5)$ V and $V_{rf} = 1061(32)$ V.

The trap was mounted onto a ceramic chip carrier, with gold ribbon wire connecting the electrodes to the chip carrier bond pads. To ensure good rf grounding 820 pF capacitors were wire bonded to the static electrodes. The chip was mounted inside a UHV vacuum system at a pressure of 8.0×10^{-8} Pa. Ytterbium ions were trapped by applying an rf voltage of 455(3) V at a frequency $\Omega/2\pi = 32.2$ MHz via a helical coil resonator with Q = 160. All other electrodes were held at ground. Atomic ovens containing natural ytterbium were ohmically heated producing a neutral flux of atoms parallel to the trap surface. Atoms were resonantly ionized using a two-color photoionization process and laser cooled, with ion fluorescence imaged onto an electron multiplied CCD array [30]. The ion secular frequencies along the trap principle axes were measured to be $(\omega_{x'}, \omega_{y'}, \omega_{z'})/2\pi = (1.58, 1.47, 3.30) \pm 0.01$ MHz respectively, for an ion trapped in the top right corner of the array. Using these measurements, numerical simulations of the trap predict a trap depth of 0.42(2) eV. The ion lifetime with cooling light was ~ 90 minutes, likely limited by background collisions

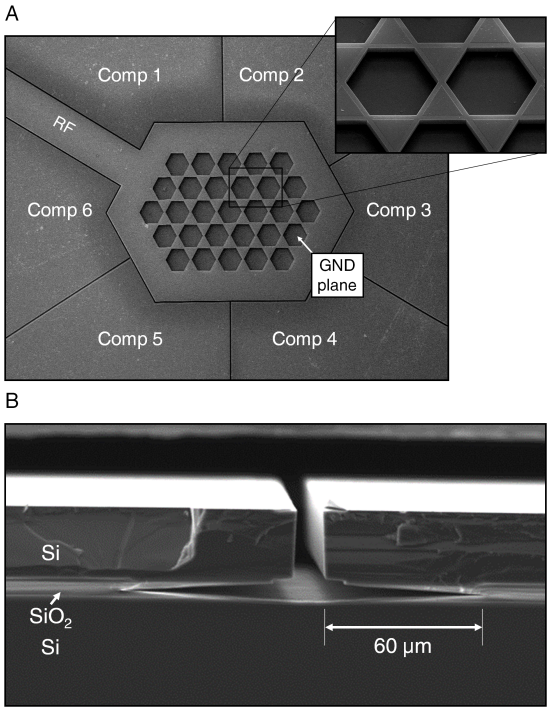

Figure 2: (**A**) An SEM of a finished microchip. The inset shows a close up of two of the hexagonal traps, this shows the recessed ground electrode. (**B**) An SEM cross section of the layered SOI structure at the interface between two compensation electrodes. The deep V-shaped undercut into the oxide layer is clearly visible extending 60 μm into the SiO_2 layer.

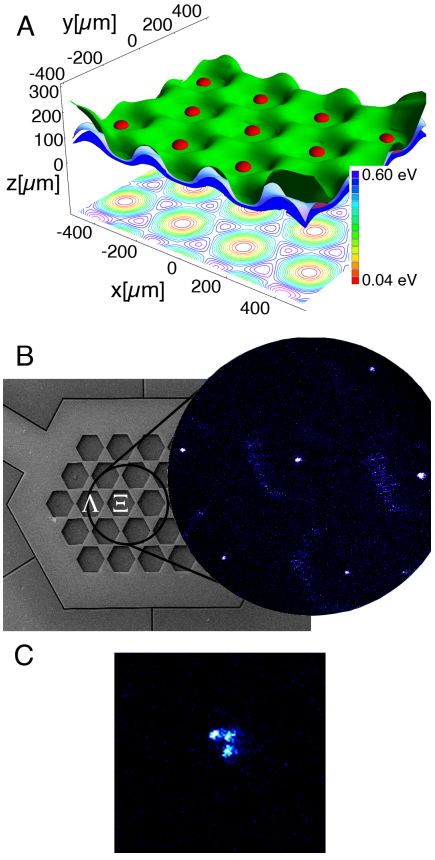

Figure 3: (**A**) A 3D contour plot of the lattice potential for the central 11 trap sites with an rf voltage of 455 V. The equipotential surfaces correspond to: red = 0.04 eV, green = 0.4 eV, light blue = 0.5 eV and blue = 0.6 eV. A 2D contour plot of the potential at the ion height is projected below, the equipotential lines are separated by 0.04 eV. (**B**) A CCD image of six ions trapped simultaneously on the lattice is shown, the hexagonal shaped electrodes are also visible due to laser scatter. The area imaged was limited by our current imaging system and marked by a black circle over an SEM image of the trap. (**C**) A CCD image of a single lattice site with a deterministically produced three-ion Coulomb crystal.

and $\gtrsim 5$ minutes without cooling light. To maximize the ion-ion coupling rate for quantum simulations, which scales as ω^{-2}, the rf voltage can be decreased to 125 V, corresponding to secular frequencies of $\omega_{x'}/2\pi \approx \omega_{y'}/2\pi \approx 0.5$ MHz. A 3D contour plot of the trap potential for the central 11 trap sites is shown in Fig. 3A, a 2D contour plot is projected below showing the potential at the ion height.

A 2D ion lattice can be seen in Fig. 3B, six ions are trapped in adjacent lattice sites, with the viewable area limited by our imaging system. If required we can deterministically expand from simulations on regular lattices by introducing defects into the lattice structure; these may include both a missing ion or the inclusion of an additional ion at a lattice site. Such defects result in an irregular lattice which when investigating Bose-Hubbard physics, such as superfluid-Mott insulator transitions, will result in site dependant phonon tunneling rates [2]. Figure 3C shows a three ion Coulomb crystal trapped in a single lattice site, this could constitute a lattice defect within a uniform lattice structure.

We have also demonstrated shuttling of ions between different sites of the lattice. An ion is initially trapped at site Ξ, as marked in Fig. 3B. By lowering the rf voltage to minimize the potential barrier and applying control voltages to the surrounding electrodes, the ion is shuttled to position Λ. Figure 4 shows two CCD images of the ion before and after shuttling, also shown are the typical shuttling voltages. To shuttle the ion back to Ξ the polarity of the voltage on Comp 3 and Comp 6 is reversed.

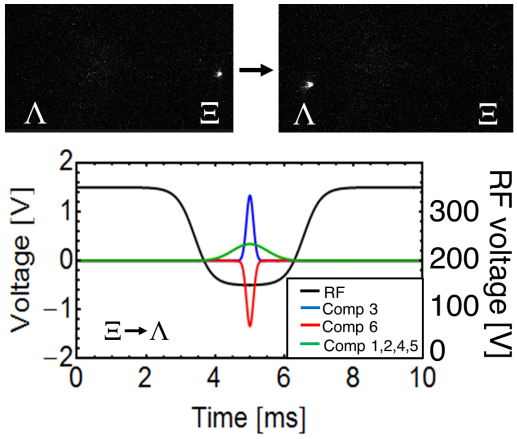

Figure 4: Two CCD images are shown before and after shuttling an ion from lattice site Ξ to Λ. The shuttling voltage profile for this shuttling operation is shown. To shuttle the ion back to Λ the polarity of the voltages on Comp 3 and 6 is reversed.

It is possible to determine the feasibility of quantum simulations that could be performed using this lattice ion trap chip. By considering the ratio β of the change in the Coulomb force to the change in the restoring force of one ion due to the displacement of a neighboring ion [21, 31], we find $\beta = 8.32$ x 10^{-6}. This indicates that ion-ion coupling is dominant between nearest neighbor ions only. Combined with a commercially available laser with a wavelength of 355 nm and a power of 20 W focused down to a 30 μm beam waist, a coupling strength $J \approx 1.1$ kHz is achievable. It is also important to consider the main sources of decoherence that can have adverse effects on the fidelity of the quantum simulation. The main source of decoherence stems from the heating rate of the ion's motional state estimated to be 1.6×10^{-11} $\mathrm{V^2 m^{-2} Hz^{-1}}$ [26], which is a function of the ion-electrode distance. K_{sim} is defined as the ratio of the heating rate to the coupling rate and is ≈ 1.05 for our ion trap lattice [31]. Additionally decoherence can result from the laser induced spontaneous emission rate which again can be compared to the coupling rate. The ratio of the coupling rate to the laser induced spontaneous emission is defined as L_{sim} [31] and is ≈ 47.9 for this laser.

The combination of a scalable microfabrication architecture for trapping 2D lattices of ions and sufficient coupling strengths between lattice sites opens up a new class of quantum simulations. A triangular lattice of trapped ions, as demonstrated here, can be used for example to explore frustrated XY models and 2D spin liquids [3]. With simple modifications to the trap geometry alternative lattice configurations such as square or honeycomb lattices, of the type recently described for the investigation of gauge fields and the fractional quantum Hall effect [4, 5], can be formed. Work to improve the ion coupling rates and local ion control will further the suitability of this trap for quantum simulation, but represent only incremental fabrication and trap design steps.

By allowing high voltages, enabling large ion-electrode separations and long ion lifetimes on a microfabricated and scalable lattice geometry, our device provides an exciting platform for the implementation of analog 2D quantum simulations using trapped ions. Not only is this lattice suitable for quantum simulations however, other applications may include the generation of 2D cluster states for ion trap quantum computing.

This work is supported by the UK Engineering and Physical Sciences Research Council (EP/E011136/1, EP/G007276/1), European Commission's Seventh Framework Programme (FP7/2007-2013) under grant agreement no. 270843 (iQIT), the European Commission's Sixth Framework Marie Curie International Reintegration Programme (MIRG-CT-2007-046432), the Nuffield Foundation and the University of Sussex.

[1] Feynman, R. P. *Int. J. Theor. Phys.* **21**, 467–488 (1982).
[2] Johanning, M., Varón, A. F., and Wunderlich, C. *J. Phys. B: At. Mol. Opt. Phys.* **42**, 154009 (2009).
[3] Schmied, R., Roscilde, T., Murg, V., Porras, D., and Cirac, J. I. *New J. Phys.* **10**, 045017 (2008).
[4] Bermudez, A., Schaetz, T., and Porras, D. *New J. Phys.* **14**, 053049 (2012).
[5] Shi, T. and Cirac, J. I. *Phys. Rev. A* **87**, 013606 (2013).
[6] Bloch, I., Dalibard, J., and Nascimbène, S. *Nat. Phys.* **8**, 267–276 (2012).
[7] Aspuru-Guzik, A. and Walther, P. *Nat. Phys.* **8**, 285–291 (2012).
[8] Blatt, R. and Roos, C. F. *Nat. Phys.* **8**, 277–284 (2012).
[9] Peng, X., Zhang, J., Du, J., and Suter, D. *Phys. Rev. Lett.* **103**, 140501 (2009).
[10] Wineland, D. J. and Leibfried, D. *Laser Phys. Lett.* **8**(3), 175–188 (2011).
[11] Islam, R., Edwards, E. E., Kim, K., Korenblit, S., Noh, C., Carmichael, H., Lin, G. D., Duan, L. M., Wang, C. C. J., Freericks, J. K., and Monroe, C. *Nat. Commun.* **2**, 377 (2011).
[12] Friedenauer, A., Schmitz, H., Glueckert, J. T., Porras, D., and Schaetz, T. *Nat. Phys.* **4**, 757–761

(2008).

[13] Gerritsma, R., Lanyon, B. P., Kirchmair, G., Zähringer, F., Hempel, C., Casanova, J., García-Ripoll, J. J., Solano, E., Blatt, R., and Roos, C. F. *Phys. Rev. Lett.* **106**, 060503 (2011).

[14] Gerritsma, R., Kirchmair, G., Zähringer, F., Solano, E., Blatt, R., and Roos, C. F. *Nature* **463**, 68–71 (2010).

[15] Lanyon, B. P., Hempel, C., Nigg, D., Müller, M., Gerritsma, R., Zähringer, F., Schindler, P., Barreiro, J. T., Rambach, M., Kirchmair, G., Hennrich, M., Zoller, P., Blatt, R., and Roos, C. F. *Science* **334**(6052), 57–61 (2011).

[16] Kim, K., Korenblit, S., Islam, R., Edwards, E. E., Chang, M.-S., Noh, C., Carmichael, H., Lin, G.-D., Duan, L.-M., Wang, C. C. J., Freericks, J. K., and Monroe, C. *New J. Phys.* **13**, 105003 (2011).

[17] Islam, R., Senko, C., Campbell, W. C., Korenblit, S., Smith, J., Lee, A., Edwards, E. E., Wang, C. C. J., Freericks, J. K., and Monroe, C. *arXiv:1210.0142* (2012).

[18] Korenblit, S., Kafri, D., Campbell, W. C., Islam, R., Edwards, E. E., Gong, Z. X., Lin, G. D., Duan, L. M., Kim, J., and Monroe, C. *New J. Phys.* **14**, 095024 (2012).

[19] Britton, J. W., Sawyer, B. C., Keith, A. C., Wang, C. C. J., Freericks, J. K., Uys, H., Biercuk, M. J., and Bollinger, J. J. *Nature* **484**, 489–492 (2012).

[20] Cirac, J. I. and Zoller, P. *Nature* **404**, 579–581 (2000).

[21] Porras, D. and Cirac, J. I. *Phys. Rev. Lett.* **92**, 207901 (2004).

[22] Chiaverini, J. and Lybarger, W. E. *Phys. Rev. A* **77**, 022324 (2008).

[23] Kumph, M., Brownnutt, M., and Blatt, R. *New J. Phys.* **13**(073043) (2011).

[24] Clark, R. J., Lin, T., Brown, K. R., and Chuang, I. L. *J. Appl. Phys.* **105**(1), 013114 (2009).

[25] Raussen, R. and Briegel, H. J. *Phys. Rev. Let.* **86**(22), 5188–5191 (2001).

[26] Hughes, M. D., Lekitsch, B., Broersma, J. A., and Hensinger, W. K. *Contemp. Phys.* **52**(6), 505–529 (2011).

[27] Britton, J., Leibfried, D., Beall, J. A., Blakestad, R. B., Wesenberg, J. H., and Wineland, D. J. *Appl. Phys. Lett.* **95**(17), 173102 (2009).

[28] Stick, D., Hensinger, W. K., Olmschenk, S., Madsen, M. J., Schwab, K., and Monroe, C. *Nat. Phys.* **2**, 36–39 (2006).

[29] Sterling, R. C., Hughes, M. D., Mellor, C. J., and Hensinger, W. K. *arXiv:1208.5672* (2012).

[30] McLoughlin, J. J., Nizamani, A. H., Siverns, J. D., Sterling, R. C., Hughes, M. D., Lekitsch, B., Stein, B., Weidt, S., and Hensinger, W. K. *Phys. Rev. A* **83**, 013406 (2011).

[31] Siverns, J. D., Weidt, S., Lake, K., Lekitsch, B., Hughes, M. D., and Hensinger, W. K. *New J. Phys.* **14**, 085009 (2012).